

# Failure Analysis Using Different Transformer Models in EMTP-ATP

Dušan Medved', Martin Kanálik

*Department of Electric Power Engineering**Technical University in Košice*

Košice, Slovakia

Dusan.Medved@tuke.sk , Martin.Kanalik@tuke.sk

**Abstract**—Various transformer models can be used to analyze fault conditions occurring in the power system. In this paper, several transformer models and their influence on the fault current course at different types of short circuits are investigated. Therefore, the 3-ph ideal transformer, the 3-ph saturable transformer (with and without saturation consideration), and the label-entered transformer (BCTRAN) were selected to compare the short-circuit current results. Faults such as 1-ph short-circuit, 2-ph metal short-circuit, 2-ph ground short-circuit and 3-ph short-circuit were considered. The results were compared with the methodology given in standard STN EN 60909-0 (33 3020).

**Keywords**—transformer, EMTP-ATP, fault condition, short-circuit current

## I. INTRODUCTION

There are cases in the power system that differ from a normal operation. In some cases, it is a state that cannot be performed on real equipment for specific conditions of analysis. Therefore, methods of mathematical or physical modeling of electrical network elements are preferably used. One of the suitable, that is designed for more detailed analysis and its results may serve as a reference, is the EMTP-ATP program.

The task of this paper is to determine specific characteristics of selected transformer models in EMTP-ATP environment, to model them and to evaluate the influence of input parameters on the resulting fault current waveform.

## II. ANALYSIS OF SHORT-CIRCUIT FAULTS ON THE SECONDARY SIDE OF THE TRANSFORMER

The aim of this section will be to analyze the fault currents on the secondary side of the transformer using different transformer models in EMTP-ATP. In Fig. 1 is a simplified schematic of an electrical circuit in the case of a failure on the secondary side of the transformer. The power system in no-load operation before the fault occurs.

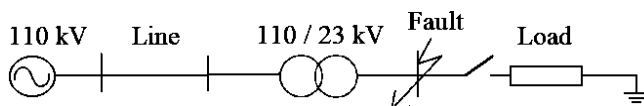


Fig. 1. Electrical circuit diagram

### Calculation of electric network elements:

Parameter	Quantity/value	Note
<i>External network</i>	$U_n = 110 \text{ kV}$	
<i>Power line</i>	$R_v = 0,025 \Omega/\text{km}$ , $X_v = 0,4 \Omega/\text{km}$ , $l = 60 \text{ km}$ , $X_{v0} = 3 \cdot X_{v1}$	
<i>Load</i>	$R_z = 150 \Omega$ , $X_{Lz} = 24 \Omega$	
<i>Transformer</i>	3-legged-stacked-core, 3-phase, 2-winding	

### Transformer parameters obtained from label data:

<i>Nominal power</i>	$S_N = 40 \text{ MVA}$	
<i>Nominal voltage</i>	$U_{N2} = 110 \text{ kV}$	Y connection
	$U_{N1} = 23 \text{ kV}$	Y connection
<i>Short-circuit voltage</i>	$u_k = 11,5 \%$	positive-sequence component
<i>Short-circuit losses</i>	$\Delta P_k = 130 \text{ kW}$	positive-sequence component at nominal current
<i>No-load losses</i>	$P_0 = 20 \text{ kW}$	positive-sequence component at nominal voltage
<i>Type of connection</i>	YNyn0(d)	

The neutral point of the secondary winding of the transformer is grounded through a resistance  $R_F = 10 \Omega$ .

In the absence of measured data for the zero-sequence component of the transformer, it is assumed that the zero-sequence component of the short-circuit reactance  $X_{0k}$  is about 85 % of the positive-sequence component of the short-circuit reactance  $X_{1k}$  (since the transformer is core type).

For Saturable Transformer Component (STC) modeling, the winding wired to the star on the lower voltage side will be referred to as winding no. 1, where the magnetizing branch and the zero-sequence branch of the magnetizing inductance are connected. Ideally, the non-linear magnetization inductance should be connected to such a point in an equivalent circuit where the integrated voltage is equal to the flow in the iron core. For cylindrical coils, it can be assumed that the winding flow will flow predominantly through the core, since there should be very little leakage.

**Parameters calculation of electrical network elements:**

Power-line:

$$R_{\text{vl}} = R_v \cdot l \cdot \frac{U_{\text{N1}}^2}{U_{\text{N2}}^2} = 0,025 \cdot 60 \cdot \frac{23^2}{110^2} = 0,06558 \Omega \quad (1)$$

$$R_{\text{v0}} = R_{\text{vl}} = 0,06558 \Omega \quad (2)$$

$$X_{\text{vl}} = X_v \cdot l \cdot \frac{U_{\text{N1}}^2}{U_{\text{N2}}^2} = 0,4 \cdot 60 \cdot \frac{23^2}{110^2} = 1,0492 \Omega \quad (3)$$

$$X_{\text{v0}} = 3 \cdot X_{\text{vl}} = 3,1472 \Omega \quad (4)$$

Transformer:

$$R_{\text{Tl}} = \frac{\Delta P_k}{S_N} \cdot \frac{U_{\text{N1}}^2}{S_N} = \frac{0,325}{100} \cdot \frac{23^2}{40} = 0,043 \Omega \quad (5)$$

$$R_{\text{T0}} = R_{\text{Tl}} = 0,043 \Omega \quad (6)$$

$$X_{\text{Tl}} = \frac{u_k}{100} \cdot \frac{U_{\text{N1}}^2}{S_N} = \frac{11,5}{100} \cdot \frac{23^2}{40} = 1,521 \Omega \quad (7)$$

$$X_{\text{T0}} = 0,85 \cdot X_{\text{Tl}} = 1,293 \Omega \quad (8)$$

Total short-circuit impedance:

$$R_1 = R_{\text{vl}} + R_{\text{Tl}} = 10,108 \Omega \quad (9)$$

$$X_1 = X_{\text{vl}} + X_{\text{Tl}} = 2,5702 \Omega \quad (10)$$

$$R_0 = R_{\text{v0}} + R_{\text{T0}} = 10,108 \Omega \quad (11)$$

$$X_0 = X_{\text{v0}} + X_{\text{T0}} = 4,4402 \Omega \quad (12)$$

$$Z_1 = R_1 + j \cdot X_1 = 0,108 + j \cdot 2,5702 = 2,572 \cdot e^{j87,59^\circ} \Omega \quad (13)$$

$$Z_0 = R_0 + j \cdot X_0 = 0,108 + j \cdot 4,4402 = 4,442 \cdot e^{j88,61^\circ} \Omega \quad (14)$$

**Calculations of short-circuit currents:**

Phase voltage amplitude on fault side:

$$U_m = \frac{\sqrt{2} \cdot U_{\text{N1}}}{\sqrt{3}} = \frac{\sqrt{2} \cdot 23}{\sqrt{3}} = 18,78 \text{ kV} \quad (15)$$

Maximum steady-state short-circuit current:

$$I_{\text{mu}} = \frac{U_m}{Z_1} = \frac{18,78}{2,572} = 7,302 \text{ kA} \quad (16)$$

Time constant of circuit:

$$t_a = \frac{L_1}{R_1} = \frac{X_1}{\omega \cdot R_1} = \frac{2,5702}{2 \cdot \pi \cdot 50 \cdot 0,108} = 0,0758 \text{ s} \quad (17)$$

RMS value of the phase voltage on the fault side:

$$E_1 = \frac{c \cdot U_{\text{v}}}{\sqrt{3}} = \frac{1 \cdot 23}{\sqrt{3}} = 13,279 \text{ kV} \quad (18)$$

Instantaneous value of short-circuit current:

$$i_k(t) = I_{\text{mu}} \cdot \sin(\omega \cdot t + \alpha - \varphi_k) + [I_{\text{m[u]}} \cdot \sin(\alpha - \varphi) - I_{\text{mu}} \cdot \sin(\alpha - \varphi_k)] \cdot e^{-\frac{t}{t_a}} \quad (19)$$

Peak current at three-phase short circuit:

$$I_p = i_k(0,01) = 7,302 \cdot [\sin(2 \cdot 180^\circ \cdot 50 \cdot 0,01 + 0^\circ - 87,59^\circ) - \sin(0^\circ - 87,59^\circ)] \cdot e^{-\frac{0,01}{0,0758}} \quad (20)$$

$$I_p = 13,689 \text{ kA} \quad (21)$$

$$(12)$$

Initial symmetrical short-circuit current at three-phase short-circuit:

$$I_{k3}'' = \left| \frac{U_{\text{v}}}{\sqrt{3} \cdot Z_1} \right| = \left| \frac{23}{\sqrt{3} \cdot 2,572} \right| = 5,163 \text{ kA} \quad (22)$$

*Initial symmetrical short-circuit current at line-to-line short-circuit:*

$$I''_{k2} = \left| \frac{U_v}{2 \cdot Z_1} \right| = \left| \frac{23}{2 \cdot 2,572} \right| = 4,471 \text{ kA} \quad (23)$$

*Input values for load:*

$$R\_1 = R\_2 = R\_3 : R_z = 150 \Omega \quad (30)$$

*Initial symmetrical short-circuit current at line-to-line with earth short-circuit:*

$$I''_{k2,1} = \left| \frac{U_v}{Z_1 + 2 \cdot Z_0 - \frac{\sqrt{3}}{2} + j \cdot \left( \frac{1}{2} + \frac{Z_0}{Z_1} \right)} \right| = 4,798 \text{ kA} \quad (24)$$

*Initial symmetrical short-circuit current at line-to-line with earth short-circuit leaked through earth.*

$$I''_{k2,1E} = 2 \cdot \sqrt{3} \cdot U_v \cdot \left| \frac{2 \cdot Z_1}{4 \cdot Z_1 \cdot (Z_1 + Z_0 + 3 \cdot R_F) + 2 \cdot Z_1 \cdot (2 \cdot Z_0 + 6 \cdot R_F)} \right| = 649 \text{ A} \quad (25)$$

*Initial symmetrical short-circuit current at line-to-earth short-circuit:*

$$I''_{k1} = \left| \frac{3 \cdot E_1}{2 \cdot Z_1 + Z_0 + 3 \cdot Z_F} \right| = \left| \frac{39,837}{31,8} \right| = 1,253 \text{ kA} \quad (26)$$

*Setting the parameters of electrical circuit elements in ATP*

Required input values must be entered for electrical circuit elements. The transformer parameter settings are shown below.

*Input values for power lines:*

$$R\_1 = R\_2 = R\_3 : R_v = R_l \cdot l = 0,025 \cdot 60 = 1,5 \Omega \quad (27)$$

$$L\_1 = L\_2 = L\_3 : X_v = X_l \cdot l = 0,4 \cdot 60 = 24 \Omega \quad (28)$$

*Input values for source:*

$$\text{Amp: } U_m = \frac{\sqrt{2} \cdot 110}{\sqrt{3}} = 89,815 \text{ kV}, f = 50 \text{ Hz} \quad (29)$$

### Case 1: Ideal three-phase transformer

In Fig. 2 is shown an electrical circuit for a case of three-phase short circuit. For another type of fault, the circuit is only modified at the fault location. Since this type of transformer does not consider its impedance, it is necessary to connect the model impedance in series, in which we enter the transformer parameters according to previously mentioned. The secondary side of the transformer is grounded through a  $10 \Omega$  resistor.

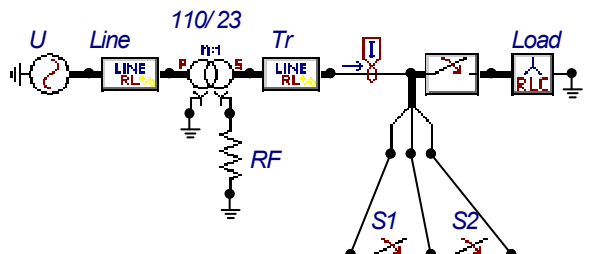


Fig. 2. Connection of electrical circuit in ATP

### Case 2: General 2-winding 3-phase saturation transformer (no saturation)

Fig. 3 shows circuit with 2-winding, 3-phase saturation transformer, where a three-phase short circuit occur. The parameters for the transformer were calculated according to the formulas mentioned bellow.

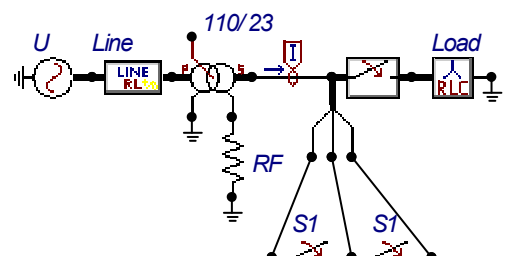


Fig. 3. Connection of electrical circuit in ATP

*Nominal current (related to the higher voltage side):*

$$I_{N2} = \frac{S_{NT}}{\sqrt{3} \cdot U_{N2}} = 209,95 \text{ A} \quad (32)$$

Total short-circuit resistance (related to the higher voltage side):

$$R_{k2} = \frac{\Delta P_k}{3 \cdot I_{N2}^2} = 0,9831 \Omega \quad (33)$$

Winding 1: connected to Y (with voltage of  $\frac{23}{\sqrt{3}} \text{ kV}$ )

Winding 2: connected to Y (with voltage of  $\frac{110}{\sqrt{3}} \text{ kV}$ )

$$R_1 = 0,2 \cdot \frac{23^2}{110^2} \cdot R_{k2} = 0,008596 \Omega \quad (37)$$

Total short-circuit impedance:

$$Z_{k2} = \frac{u_k \cdot U_{N2}^2}{S_N} = 34,7875 \Omega \quad (34)$$

$$X_1 = 0,2 \cdot \frac{23^2}{110^2} \cdot X_{k2} = 0,304 \Omega \quad (38)$$

$$R_2 = 0,8 \cdot R_{k2} = 0,78648 \Omega \quad (39)$$

Total short-circuit reactance:

$$X_{k2} = \sqrt{Z_{k2}^2 - R_{k2}^2} = 34,7736 \Omega \quad (35)$$

$$X_2 = 0,8 \cdot X_{k2} = 27,8189 \Omega \quad (40)$$

No-load loss resistance (lower voltage side):

$$R_{mag} = 3 \cdot \frac{U_{N1}^2}{P_0} = 79,35 \text{ k}\Omega \quad (36)$$

The transformer is 3-legged stacked core type, so the homopolar magnetization resistance is high and  $\frac{X_{0k}}{X_{1k}} = 0,85 \leq 1$ . The zero-sequence component of magnetization inductance  $L_{0mag}$  (on the lower voltage side) required for the STC model is to be retrospectively determined.

An equivalent circuit for the zero-sequence component of the transformer, related to the higher voltage winding, is given in Fig. 5.

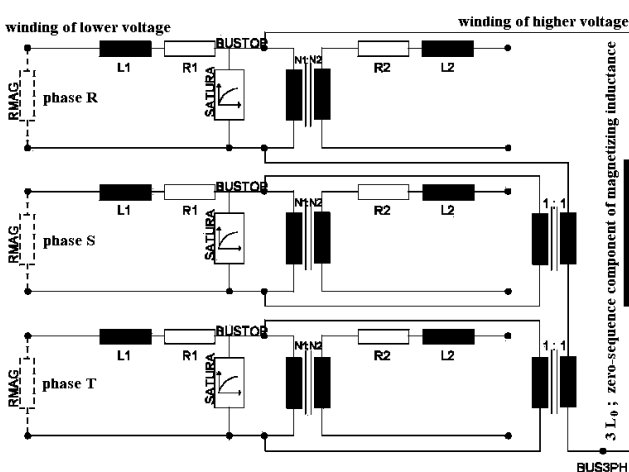


Fig. 4. 2-winding, 3-phase saturation transformer with zero-sequence component of magnetizing inductance

In fact, the total short-circuit impedance is distributed unevenly between the primary and secondary windings. Here is the ratio  $\frac{1}{4}$  for  $\frac{Z_{k1}}{Z_{k2}}$ . The required data for the STC model (see Fig. 4) can be determined from the above values:

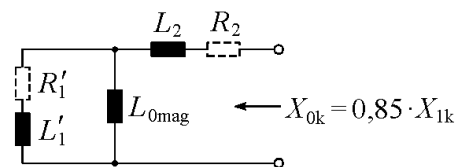


Fig. 5. Equivalent circuit for  $L_{0mag}$  calculation

In Fig.,  $R'_1$  a  $L'_1$  are the winding impedances on the lower voltage side and are related to the higher voltage winding. When determination of  $L_{0mag}$ , the resistances  $R'_1$  a  $R_2$  are neglected because  $R'_1 \ll X'_1$  and  $R_2 \ll X_2$ .

$$X'_1 = 0,2 \cdot X_{k2} = 6,95472 \Omega \quad (41)$$

$$\frac{1}{X'_{0mag}} = \frac{1}{X_{0k} - X_2} + \frac{1}{X'_1} \Rightarrow X'_{0mag} = 1,391 \Omega \quad (42)$$

$$L_{0mag} = \frac{U_{N1}^2 \cdot X'_{0mag}}{U_{N2}^2 \cdot \omega} = \frac{23^2}{110^2} \cdot \frac{1,391}{2 \cdot \pi \cdot 50} = 0,19367 \text{ mH} \quad (43)$$

(related to the winding on the lower voltage side)

EMTP-ATP also expects the value of magnetic resistance  $R_0$  with the unit as input of  $\frac{\text{kV}^2}{\text{H}}$ :

$$R_0 = \frac{U_{\text{N1}}^2}{3 \cdot L_{0\text{mag}}} = 910483 \frac{\text{kV}^2}{\text{H}} \quad (44)$$

Finally, the linear magnetization inductance for the SATURA branch can be defined using the first pair of data (0.412 A, 18584 V) from the positive-sequence component measurement by specifying current  $I$  and flux (steady state):

$$i = \sqrt{2} \cdot 0,412 \text{ A} = 0,5827 \text{ A} \quad (45)$$

$$\psi = \frac{\sqrt{2} \cdot U}{\omega} = 83,7 \text{ V} \cdot \text{s} \quad (\text{note: } [\text{V} \cdot \text{s}] = [\text{Wb}]) \quad (46)$$

### Case 3: General 2-winding 3-phase saturation transformer (with saturation)

The connection scheme in the ATP and the input values for this type are the same as the previous type (Case 2). In addition, the saturation curve (Fig. 6) according to Table 1 is entered.

TABLE I. INPUT VALUES FOR THE SATURATION CURVE

$I$ [A] RMS	$U$ [V] RMS
0.412	18584
0.492	20677
0.723	23046
1.084	24262
2.269	25691

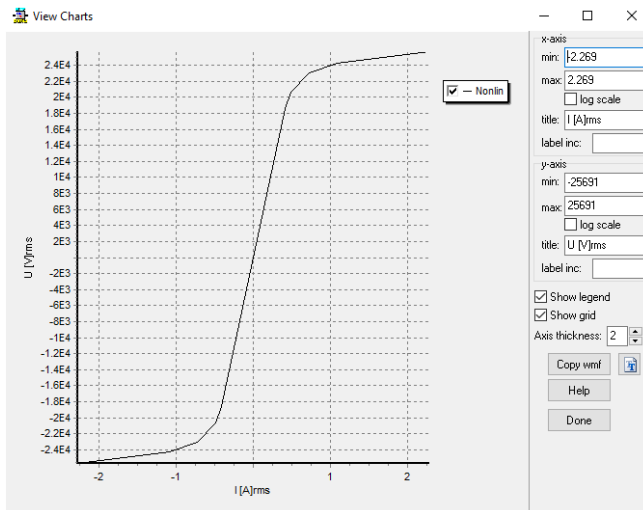


Fig. 6. Plotting of saturation curve

### Case 4: Transformer of BCTRAN model

The electrical circuit for the three-phase short-circuit is shown in Fig. 7. In this type, we also enter values from measurements according to Fig. 8.

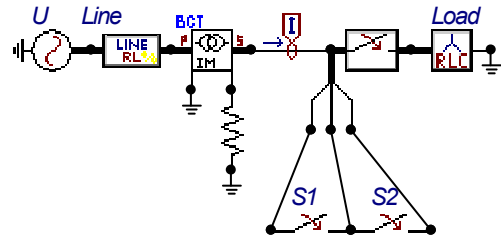


Fig. 7. Connection of electrical circuit in ATP

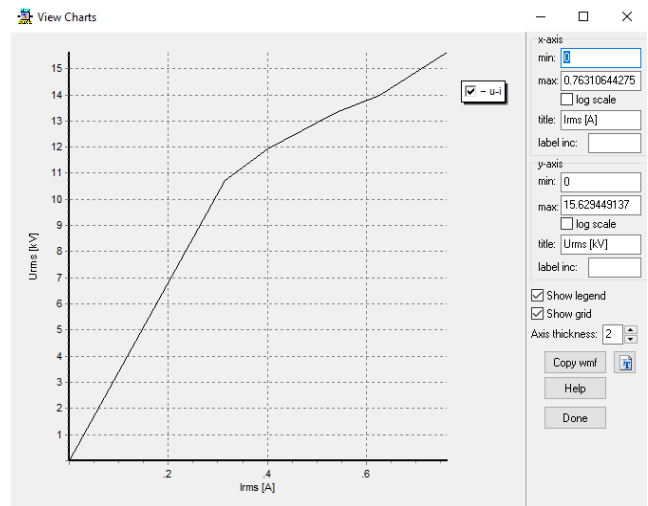


Fig. 8. Plotting of magnetization curve

### III. COMPARISON OF THE RESULTING SHORT-CIRCUIT CURRENT VALUES

The resulting values obtained from the simulations and calculations are given in the following Table 2. From the resulting waveforms, it is possible to determine peak current values and maximum short-circuit current values for various types of short-circuits. In simulations, it is assumed that the short circuit occurred at 0.1 s. Thus, the peak current was expected at 0.11 sec. The maximum values of steady-state short-circuit currents were re-calculated to RMS values and put in the Table 2.

TABLE II. RESULTING VALUES OF SHORT-CIRCUIT CURRENTS

Short-circuit type	3-ph	3-ph	2-ph	2-ph-E	2-ph-E	1-ph
Transformer type	A-B-C	A-B-C	B-C	B-C-N	B-C-N	A-N
Calculated values	13689	5163	4471	4798	649	1253
Ideal transf. (TRAFO I3)	13638	5164	4470	4785	649	1252
Transformer GENTRAFO (no satur.)	13705	5165	4469	4786	648	1247
Transformer GENTRAFO (with satur.)	13609	5280	4470	4785	646	1256
Transformer BCTRAN	13706	5166	4472	4787	647	1250

#### IV. CONCLUSION

For the particular types of faults (three-phase, line-to-line, line-to-line with earth and line-to-earth short-circuit), the fault currents during the operation of power system using of different transformer models available in EMTP-ATP were examined in the this paper.

The resulting values obtained by calculation correspond most to the ideal three-phase transformer, in which only the transformer ratio and the effective impedance with calculated transformer parameters were entered.

However, the BCTRAN and GENTRAFO transformers are the most appropriate for the real situation. It is because for these types we entered several parameters obtained from measurements, such as type of transformer core, type of connection and phase shift, but especially values obtained from transformer tests (no-load and short-circuit measurements for positive-sequence or possibly zero-sequence component) or parameters were entered on the basis of calculations.

The recorded fault current values were compared with the calculated values given in Table 2.

For all types of faults, the simulation deviations from the calculated values were minimal for all transformer models used (less than 0.5 %).

The minimal differences in these values confirm the qualities of the EMTP-ATP program, which can be used as a reference for calculations of a similar kind.

The use of computer technology to solve transient phenomena with suitable software is an advantage that allows to improve the overview of the conditions and situations in the power system. It is thus possible to obtain a clear idea of the function of individual components of the solved electrical networks and thus of the influence of a particular component on the behavior of the network as a whole. This knowledge can be extended by examining networks under changed conditions of global parameters, but also parameters valid for individual elements of the studied circuits, which is advantageous especially for large circuits.

The use of the EMTP-ATP program may already be directly in the projection and designing, where the proposed solutions can be verified in advance both in steady-state operation and in simulation of transient phenomena. An indisputable advantage is to get an almost instantaneous overview of the sizes, waveforms and frequencies of currents and voltages in any branch and network node. The program also allows obtaining power values in nodes and elements of the modeled circuit. The results when simulating transient phenomena in the form of short-circuit currents or overvoltage sizes can be used to design current or overvoltage protections. The program can also be used to investigate the stability of the power system, for example, so that circuit simulation results can be input for other computing programs that already offer static or dynamic stability calculation.

#### ACKNOWLEDGMENT

This work was supported by the Ministry of Education, Science, Research and Sport of the Slovak Republic and the

Slovak Academy of Sciences under the contract No. VEGA 1/0372/18.

#### REFERENCES

- [1] International Renewable Energy Agency, “Off-grid renewable energy systems: status and methodological issues”, [online]. Available at: <[https://www.irena.org/DocumentDownloads/Publications/IRENA\\_Off-grid\\_Renewable\\_Systems\\_WP\\_2015.pdf](https://www.irena.org/DocumentDownloads/Publications/IRENA_Off-grid_Renewable_Systems_WP_2015.pdf)>.
- [2] A. H. Hajimiragha, M. R. D. Zadeh, “Research and development of a microgrid control and monitoring system for the remote community of Bella Coola”, IEEE International Conference on Smart Energy Grid Engineering. E-ISBN 978-1-4799-2775-3.
- [3] Myomin T., et. al., “Investigation of EMTP transformer model for TRV calculation after fault current interrupting by using FRA measurement”, In: IEEE PES T&D 2010, DOI: 10.1109/TDC.2010.5484252, ISSN: 2160-8555.
- [4] STN EN 60909-0, “Short-circuit currents in three-phase a.c. systems - Part 0: Calculation of currents”.
- [5] D. Medved, M. Kanalik, “Measurement of power quality on the COTEK S1500-124 Inverter's terminals in case of linear load supplying”, In: Universal Journal of Electrical and Electronic Engineering. Vol. 2, no. 4 (2014), p. 178-182. ISSN 2332-3280.
- [6] J. Zbojovský, M. Pavlík, “Calculating the shielding effectiveness of materials based on the simulation of electromagnetic field”, In: Elektroenergetika 2017. Košice: TU, 2017 p. 369-372. ISBN 978-80-553-3195-9.
- [7] M. Pavlík, et. al., “The impact of electromagnetic radiation on the degradation of magnetic ferrofluids”, In: Archives of Electrical Engineering. Vol. 66, no. 2 (2017), p. 361-369. ISSN 1427-4221.
- [8] D. Rot, J. Jirinec, J. Kozeny, A. Podhrazky, J. Hajek, S. Jirinec, “Induction system for hardening of small parts”. In Proceedings of the 2018 19th International Scientific Conference on Electric Power Engineering (EPE). Piscataway: IEEE, 2018, p. 277-282. ISBN: 978-1-5386-4612-0, ISSN: 2376-5623.
- [9] D. Rot, J. Kozeny, S. Jirinec, J. Jirinec, A. Podhrazky, I. Poznyak, “Induction melting of aluminium oxide in the cold crucible”, In: 18th International Scientific Conference on Electric Power Engineering (EPE) 2017, pp 1-4, DOI: 10.1109/EPE.2017.7967281.
- [10] K. Nohac, M. Tesarova, L. Nohacova, J. Veleba, V. Majer, “Utilization of Events Measured by WAMS-BIOZE-Detector for System Voltage Stability Evaluation”, IFAC-PapersOnLine, Volume 49, Issue 27, 2016, pp 364-369, DOI: 10.1016/j.ifacol.2016.10.747.
- [11] M. Kolcun, M. Kornatka, A. Gawlak, Z. Conka, „Benchmarking the reliability of medium-voltage lines“, In: Journal of electrical engineering, Vol. 68, Issue: 3, Pages: 212-215, 2017, DOI: 10.1515/jee-2017-0031, ISSN: 1335-3632.
- [12] J. Dzmura, J. Petras, J. Balogh, J. Kurimsky, R. Cimbala, I. Kolcunova, B. Dolnik, M. Kolcun, “Separation of solid particles from flowing gases by AC high voltage”, In: Journal of electrostatics, Vol. 88, Elsevier Science BV, 2017, pp. 158-164, ISSN: 0304-3886.
- [13] J. Zbojovsky, M. Pavlik, Z. Conka, L. Kruzelak, M. Kosterec, “Influence of shielding paint on the combination of building materials for evaluation of shielding effectiveness”. In: EPE 2018. Brno: Univ. of Technology, 2018, pp. 324-327. ISBN 978-1-5386-4611-3.
- [14] M. Kosterec, J. Kurimsky, M. Folta, Z. Conka, S. Bucko, “Investigation of effects of non-ionizing electromagnetic fields interacting with biological systems”, In: 8th Int. Sci. Symposium on Electrical Power Engineering (Elektroenergetika 2015), p 564-567.
- [15] Z. Eleschova, A. Belan, B. Cintula, B. Bendik, “Smart grids analysis – View of the transmission systems voltage stability”, In EPE 2018. Brno: Univ. of Techn., 2018, pp. 37-42. ISBN 978-1-5386-4612-0.
- [16] D. Kapral, P. Bracinik, M. Roch, M. Hoger, “Optimization of distribution network operation based on data from smart metering systems”, Electrical Engineering, Vol. 99, Issue 4, Springer, New York, USA, 2017, December, pp: 1417-1428, ISSN 0948-7921.
- [17] M. Špes, L. Beňa, M. Kosterec, M. Márton, “Determining the current capacity of transmission lines based on ambient conditions”, In: Journal of Energy Technology. Vol. 10, no. 2 (2017), p. 61-69. ISSN 1855-5748.